

# S-L1: A Software-based GPU L1 Cache that Outperforms the Hardware L1 for Data Processing Applications

Reza Mokhtari and Michael Stumm  
Department of Electrical and Computer Engineering  
University of Toronto  
Toronto, Canada  
{mokhtari, stumm}@ece.toronto.edu

## ABSTRACT

Implementing a GPU L1 data cache entirely in software to usurp the hardware L1 cache sounds counter-intuitive. However, we show how a software L1 cache can perform significantly better than the hardware L1 cache for data-intensive streaming (i.e., “Big-Data”) GPGPU applications. Hardware L1 data caches can perform poorly on current GPUs, because the size of the L1 is far too small and its cache line size is too large given the number of threads that typically need to run in parallel.

Our paper makes two contributions. First, we experimentally characterize the performance behavior of modern GPU memory hierarchies and in doing so identify a number of bottlenecks. Secondly, we describe the design and implementation of a software L1 cache, S-L1. On ten streaming GPGPU applications, S-L1 performs 1.9 times faster, on average, when compared to using the default hardware L1, and 2.1 times faster, on average, when compared to using no L1 cache.

## 1. INTRODUCTION

We are interested in using Graphical Processing Units (GPUs) to accelerate what in the commercial world is popularly referred to as “big data” computations. These computations are dominated by functions that filter, transform, aggregate, consolidate, or partition huge input data sets. They typically involve simple operations on the input data, are trivially parallelizable, and the input data exhibits no (or very low) reuse. In the GPU world these type of computations are referred to as *streaming computations*.

GPUs appear to be ideal accelerators for streaming computations: with their many processing cores, today’s GPUs have 10X the compute power of modern CPUs, and they have close to 6X the memory bandwidth of modern CPUs,<sup>1</sup>

<sup>1</sup>For example, Nvidia GTX Titan Black has 5.1 TFLOPS of compute power and 336 GB/s of memory bandwidth,

yet are priced as commodity components.

However, a number of issues had until recently prevented effective acceleration in practice. GPUs and CPUs have separate memories so that the input data must first be copied over to the GPU, causing extra overhead [6]. The PCIe link that connects the two memories has limited bandwidth and transferring data over the PCIe bus at close to theoretically maximum bandwidth is non-trivial. Finally, the high GPU memory bandwidth can only be exploited when GPU threads, executing simultaneously, access memory in a *coalesced* fashion, where the accessed memory locations are adjacent to each other. Our recent research efforts have mitigated these issues to a large extent. For example, we were able to obtain speedups on seven realistic streaming computations of between 0.74 and 7.3 (3.0 avg.) over the most efficient CPU multicore implementations and between 4.0 and 35.0 (14.2 avg.) over the most efficient single CPU core implementations [14].

These efforts have shifted the primary bottleneck preventing higher GPU core utilization from the PCIe link to the GPU-side memory hierarchy. In particular, three factors currently prevent further improvements in core utilization. First, the GPU L1 caches are inefficient [8]. For the number of cores typical in modern GPUs, the L1 caches are too small and their cache line sizes are disproportionately large given the small cache size. For example, the L1 on the Nvidia GTX Titan Black we used to run our experiments can be configured to be at most 48KB per 192 cores and the cache line size is 128B. At best, this leaves just two cache lines per core. Yet GPGPU best practices expect many threads to run simultaneously per core, each having multiple memory accesses in-flight (supported by 340 4-byte registers per core). With the large number of executing threads, each issuing multiple memory accesses, cache lines are evicted before there is any reuse, causing a high degree of cache thrashing and attendant low L1 hit rate. As an example, Figure 1 depicts the L1 hit rate as a function of the number of threads executing when running the Unix word count utility, *wc*.

The hardware L1 has proven to be so ineffective that some recent GPU chip sets (e.g. Nvidia GTX Titan Black) by default disable the L1 caching of application data. We do not expect GPU L1 caches to become significantly more effective any time in the near future, given historical trends (see

while Intel Haswell has 500 GFLOPS of compute power and 52 GB/s of memory bandwidth.

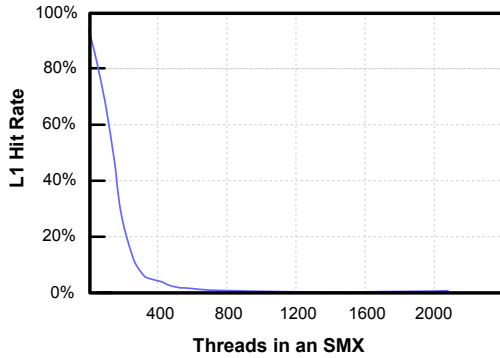


**Figure 1:** L1 hit rate when running `wc` on Titan Black GPU with 192 cores. The target data is partitioned into  $n$  chunks with each chunk assigned to a thread for processing. With a small number of threads, caching is effective, as the first access of each thread results in a miss, but the subsequent 127 accesses result in cache hits. With a large number of threads, 128 accesses can result in 128 misses. Section 2.2).

A second factor preventing further improvements in core utilization is the high latency to access L2 and DRAM. On the Nvidia GeForce GTX Titan Black, the latency of a single, isolated access to L2 and DRAM is 240 and 350 cycles, respectively. These increase substantially when the number of threads/accesses increases. Hardware multithreading can hide some of this latency, but far from all of it, as we show in Section 2.3.

Thirdly, bottlenecks on the path from L2/DRAM to GPU cores prevent scaling of memory throughput and can prevent exploitation of the full L2 and DRAM bandwidth, as we will also show in Section 2.3. Thus, for memory intensive applications, average memory access latencies will be significantly higher than the latency of single, isolated accesses.

The above three factors negatively affect the workloads we are targeting and do so in a noticeable way, because many of the big-data computations are completely memory bound and dominated by character accesses, requiring only a trivial amount of computation between accesses. The end result: extremely low GPU core utilization.

In this paper, we provide a detailed characterization of the behavior of the GPU memory hierarchy and then propose and evaluate an L1-level cache implemented entirely in software to address some of its issues. The software-L1 cache (S-L1) is located in software-managed GPU *shared memory*, which is positioned at the same level as the L1, has the same access latency as the L1 (80 cycles on the Nvidia GTX Titan Black), and is also small (max. 48KB per GTX Titan Black multiprocessor). We use compiler to automatically insert the code required to implement S-L1, so S-L1 does not require modifications to the GPU application code.

The design of S-L1 is guided by three key principles to deal with the small size of the shared memory:

1. **Private cache segments:** S-L1 is partitioned into thread-private cache lines, instead of having all threads

share the cache space;

2. **Smaller cache lines:** the cache-line size is chosen to be 16B, which is less than the 128B that is typical in GPUs, and is thus able to serve a larger number of threads effectively;
3. **Selective caching:** S-L1 caches only the data of only those data structures where caching is most effective.

The objective of this design is to significantly decrease average memory access times and reduce cache thrashing. It is implemented entirely in software using a fairly straightforward runtime scheme where the code to manage and use the cache is added by using simple compiler transformations. The specific parameters of the S-L1 cache are determined at runtime during an initial brief monitoring phase, which also identifies the potential cache hit rate of each data structure. After the monitoring phase, the computation is executed using the S-L1 cache for the data structures expected to have a sufficiently high cache hit rate, given the determined amount of cache space available to each thread.

In our experimental evaluation using ten GPU-local applications, S-L1 achieves an average speedup of 1.9 over hardware L1 and an average speedup of 2.1 over no L1 caching. The speedup on hardware L1 ranges from a slowdown of 0.14 to a speedup of 4.3, and the speedup on no L1 ranges from a slowdown of 0.05 to a speedup of 6.5. These speedups are achieved despite the fact that each memory access requires the additional execution of at least 4 instructions (and up to potentially hundreds of instructions) when running S-L1. Combining S-L1 with BigKernel, the fastest known technique accelerating GPU applications processing large data sets initially located in CPU memory [14], leads to an average speedup of 1.19 over BigKernel alone, and an average speedup of 3.7 over the fastest CPU multicore implementation of the same applications. The speedup on BigKernel alone ranges from 1.04 to 1.45 and the speedups on the CPU implementations range from 1.3 to 6.37.

This paper makes the following two specific contributions:

1. we characterize the performance behavior of the GPU memory hierarchy and identify some of its bottlenecks using a number of experiments, and
2. we propose S-L1, a level-1 cache implemented entirely in software and evaluate its performance; novel features of S-L1 include a run-time scheme to automatically determine the parameters to configure the cache, selective caching, and thread-specific cache partitions.

It should be noted that S-L1 is designed and effective only for a specific workload we are targeting; other workloads may well require different design parameters or not benefit from a software implementation at all. S-L1 can be enabled/disabled on a per application basis. While a software implementation of the L1 cache adds considerable base overhead that has to be amortized, having the implementation be in software allows easier customization.

Our paper is organized as follows. Section 2 describes background information about GPUs, some architectural trends we have observed over the past few years, and the micro-architectural behavior that motivated us to do this work. We described the design and implementation of S-L1 in Section 3 and present the results of our experimental performance evaluations in Section 4. Section 5 discusses related work, and we close with concluding remarks in Section 6.

## 2. BACKGROUND

We first describe the architecture of the Nvidia GTX Titan Black to provide a brief overview of typical current GPU architectures. This subsection can be skipped by readers already familiar with GPU architectures.

We then present several GPU architectural trends to provide insight as to where future GPU architectures might be headed, and then use these trends to motivate our S-L1 cache implementation.

Finally, we present several limitations of the GPU memory hierarchy and offer some insights into the nature of those limitations, further motivating our S-L1 design.

### 2.1 GPU Background

Figure 2 shows the high-level architecture of the Nvidia GTX Titan Black. We describe this particular chip because it was used in our experimental evaluation, but also because it is representative of current GPUs. In particular, the most recent offering by Nvidia, the GTX Titan X uses the same basic Kepler architecture [23], although the number of cores, memory/cache sizes, and some micro-architectural details will differ.

The GTX Titan Black consists of fifteen *streaming multiprocessors* (SMX), each of which contains 192 computing cores, 64K 4-byte registers, 16KB-48KB L1 cache and 16KB-48KB software managed on-chip memory called *shared memory*, accessible to all cores of the SMX.<sup>2</sup> A 1.5MB L2 cache is shared by all SMXs, and the L2 cache is connected to 6GB DRAM memory called *global memory*. We refer to this global memory as *GPU memory* in this paper to differentiate it from CPU main memory. Access latency to registers, L1, shared memory, L2 and DRAM is 10, 80, 80, 240, and 350 cycles, respectively. The theoretically maximum bandwidth from L1 (per SMX), shared memory (per SMX), L2 and DRAM have been reported as 180.7GB/s, 180.7GB/s, 1003GB/s, and 336GB/s, respectively [21].

The term *kernel* is used to denote the function that is executed on the GPU by a collection of threads in parallel. The programmer specifies the number of threads to be used, grouped into *thread blocks*, with a maximum of 1,024 threads per thread block. Each thread block is assigned to a SMX by a hardware scheduler. Each SMX can host up to a maximum of 2,048 running threads (e.g. two full-sized thread blocks) at a time.

Threads of a thread block are further divided into groups of

<sup>2</sup>Each SMX also contains a texture cache and a constant cache, but they are not relevant for our objectives and hence not considered in this paper.

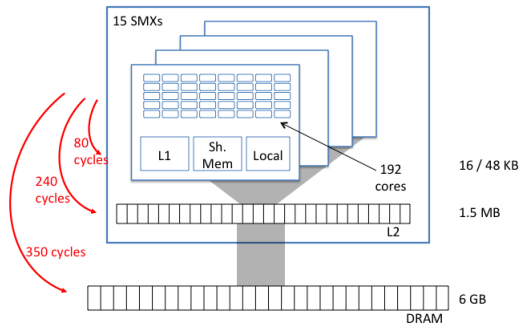


**Figure 2:** Architecture of the Nvidia GTX Titan Black.

32, called *warps*. The threads in a warp execute in lock-step because groups of 32 cores share the same instruction scheduler. This lock-step execution will lead to *thread divergence* if, on a conditional branch, threads within the same warp take different paths. Thread divergence can lead to serious performance degradations.

The memory requests issued by threads of a warp that fall within the same aligned 128-byte region are coalesced into one memory request by a hardware *coalescing unit* before being sent to memory, resulting in only one 128-byte memory transaction. Parallel memory accesses from a warp to data are defined as *n-way coalesced* if *n* of the accesses fall within the same aligned 128-byte region.

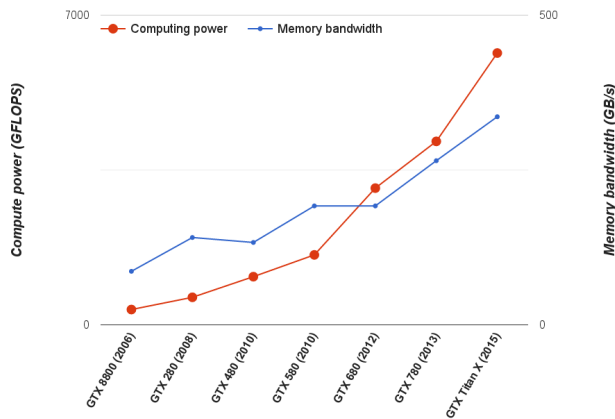
### 2.2 Historical Trends

Figure 3 depicts how Nvidia GPU aggregate compute power (in GFLOPS) and memory bandwidth (in GB/s) have evolved over chip generations, from their earliest CUDA-enabled version to the current version. Compute power has been increasing steadily at a steep slope. Memory bandwidth has also been increasing, but not as quickly. As a result, memory bandwidth per FLOP has decreased by a factor of 5: from 250 bytes/KFLOP for the GTX 8800 to 54 bytes/KFLOP for the GTX Titan X.

Figure 4 depicts how aggregate compute power and total size of fast on-chip memory (L1 cache and shared memory) have evolved over time. The total amount of on-chip memory varies over time and at one point even decreases substantially from one generation to the next. It has clearly not kept up with the increase in compute power.

If these trends continue then the GPU cores will become increasingly memory starved. Strategies to optimize GPU applications to make more efficient use of the memory hierarchy will likely become more important going forward.

Given the fact that future GPU generations may have smaller on-chip memory sizes, as has happened in the past, GPU programmers cannot assume the availability of a specific shared memory size. As a result, the programmer will need to design GPU applications so that they configure the use of shared memory at run-time and possibly restrict the number of threads used by the application. Or use run-time



**Figure 3:** Compute power and memory bandwidth over time/GPU generation.

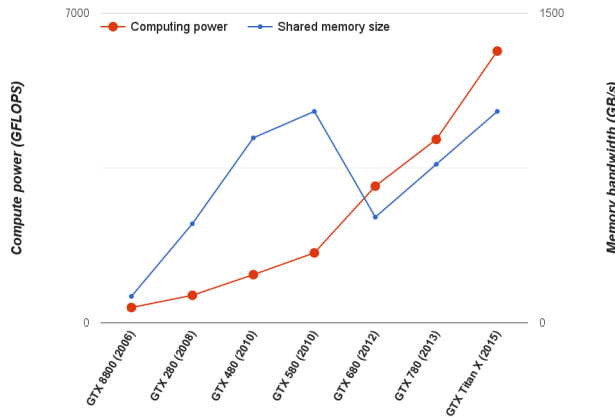


**Figure 4:** Compute power and L1 / shared memory size over time/GPU generation.

libraries, such as the one we are presenting in this paper, that automatically adjust program behavior to the available hardware resources.

## 2.3 Behavior of GPU memory access performance

GPU vendors do not disclose much information on the micro-architecture of their GPUs. Hence, in order to optimize GPGPU programs so that they can more efficiently exploit hardware resources, it is often necessary to reverse engineer the performance behavior of the GPUs through experimentation. In this section, we present the results of some of the experiments we ran to gain more insight into the memory subsystem. All results we present here were obtained on an Nvidia GTX Titan Black.

### 2.3.1 Memory access throughput

In our first set of experiments, we used a micro-benchmark that has threads read disjoint (non-contiguous) subsets of

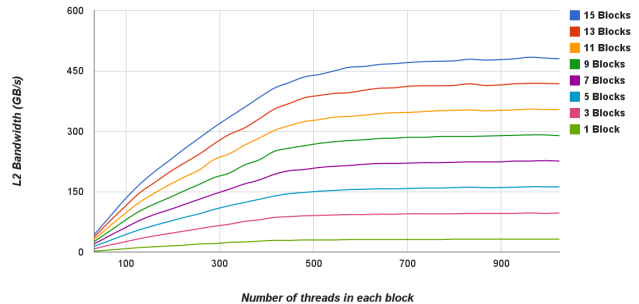


**Figure 5:** L2 memory throughput as a function of number of threads in a thread block. Each curve represents the throughput for a different number of thread blocks (1 to 15) with each thread block running 1,024 threads.

data located in the L2 cache as quickly as possible. The benchmark is parameterized so that the degree of coalescing can be varied. Figure 5 shows the maximum L2 memory bandwidth obtained, measured as the number of bytes transferred over the network, when servicing 4-way coalesced accesses from the L2 cache as the number of threads running in each thread block is increased up to 1,024.

Each curve represents a different number of thread blocks used, and each block uses the same number of threads. The thread blocks are assigned to SMXs in a round robin manner by the hardware. Focusing on the bottom curve, representing an experiment that has just one thread block running on one SMX, one can see that the memory throughput flattens out after about 512 threads at slightly less than 32 GB/s.<sup>3</sup> We observe similar behavior for DRAM (not shown) when we adjusted the micro-benchmarks to only access data certain to not be in the L2 cache, except that the throughput flattens out earlier at about 480 threads, reaching to a peak bandwidth of 307 GB/s with 15 blocks.

It is difficult to assess what causes the stagnation in L2 and DRAM throughput. However the near-linear scalability with the number of thread blocks indicates that the bottleneck is in the interconnect or in the SMX itself (e.g., coalescing units) rather than L2 or DRAM. This is shown in Figure 6 where we show the throughput as a function of the number of thread blocks with each thread block running 1,024 threads. Each point along the L2 bandwidth curve is equal to the end point (at 1,024 threads) of the corresponding curve of Figure 5. L2 throughput increases almost linearly, reaching close to 480 GB/s with 15 blocks. DRAM throughput increases almost linearly up to 10 thread blocks at which point the bandwidth limits at around 300GB/s.

The above results measured the amount of data transferred to the SMXs by the hardware. In practice, however, much of this data may not actually be used by the application. For example, for non-coalesced accesses, each 4-byte integer

<sup>3</sup>Our experiments show that varying the degree of coalescing does not completely remove the flattening out behavior. However, the smaller the coalescing degree (e.g. 1-way coalesced), the earlier the curve flattens out.

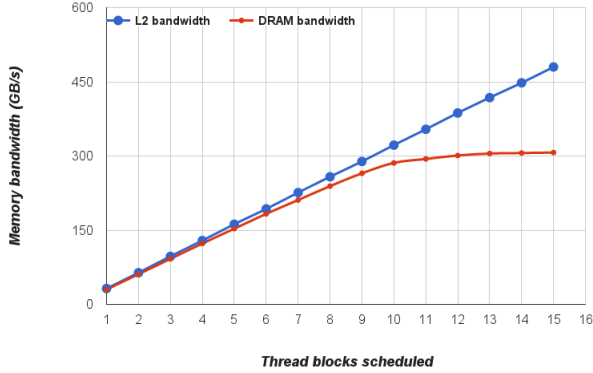


**Figure 6:** L2 and DRAM memory bandwidth as a function of number of thread blocks where each thread block is running 1,024 threads and the memory accesses are 4-way coalesced.

access will result in 32 byte transfer, of which only 4 are actual used.

The end result is that the memory access latencies actually experienced in practice will be far larger than the theoretical access latencies presented in Section 2.1. This implies that an SMX-local L1 cache, whether implemented in hardware or software, can dramatically reduce the average latency of accesses with locality, if implemented appropriately. In particular, in contrast to L2 and DRAM throughput, shared memory throughput within an SMX (not shown) does not flatten out and reaches 60GB/s (for an aggregate throughput of close to 900GB/s with 15 SMXs).

### 3. S-L1 DESIGN AND IMPLEMENTATION

#### 3.1 Overview

S-L1 is a level 1 cache implemented entirely in software. It uses the space available in each SMX’s shared memory, which has the same access latency as the hardware L1. We also considered using SMX’s texture cache, but it is a hardware-managed, read-only cache and thus, does not suit S-L1 needs.<sup>4</sup>

The design of S-L1 is based on three key design elements. First, the cache space is partitioned into thread-private cache segments, each containing one or more cache lines. The number of cache lines in each segment is determined dynamically at runtime based on the amount of available shared memory, the number of threads running in the SMX, and the size of the cache line. The decision to use thread-private cache segments is based on the fact that inter-thread data sharing is rare in the streaming applications we are targeting. Therefore, the threads mostly process data independently in disjoint locations of memory. Allowing all threads to share the entire cache space would likely result in unnecessary collisions.

Secondly, we use relatively small cache lines. The optimal

<sup>4</sup>In a separate set of experiments, we also evaluated the effectiveness of texture cache for streaming applications. The results show that, like hardware L1 cache, texture cache hit rate drops significantly when the number of online threads increase, creating a graph similar to Figure 1 (not shown).

cache line size depends to a large extent on the applications’ memory access patterns. Larger cache lines perform better for applications exhibiting high spacial locality, but they perform poorer for applications with low spacial locality due to (i) the extra overhead of loading the cache lines requiring multiple memory transactions and (ii) the increased cache thrashing because fewer cache lines are available. We decided on using 16-byte cache lines after experimenting with different cache line sizes — see Section 4.5. This size works well because 16B is the widest load/store size available on modern GPUs, allowing the load/store of an entire line with one memory access.

Thirdly, we only cache some of the application’s data structures.<sup>5</sup> The number of cache lines allocated to each thread (*CLN*) determines how many data structures we cache. *CLN* is calculated at runtime as

$$\lfloor (shMemSizePerSM / numThreadsPerSM) / cacheLineSize \rfloor$$

where *shMemSizePerSM* is the amount of shared memory available per SMX, *numThreadsPerSM* is the total number of threads allocated on each SMX, and *cacheLineSize* is the size of the cache line; i.e., 16 bytes in our current design.

The amount of shared memory available for the S-L1 cache depends on how much shared memory has previously been allocated by the application. The application can allocate shared memory statically or dynamically at run time. Hence, a mixed compile-time/runtime approach is required to identify how much shared memory remains available for S-L1. *NumThreadsPerSM* is calculated at runtime, in part by using the configuration the programmer specifies at kernel invocation and in part by calculating the maximum number of threads that can be allocated on each SMX which in turn depends on the resource usage of GPU threads (e.g. register usage) and available resources of SMX, which is extracted at compile-time and runtime, respectively.

Once the number of cache lines per thread – *CLN* – has been determined, up to that many data structures are marked as S-L1 cacheable and a separate cache line is assigned to each. In principle, multiple cache lines could be assigned to a data structure, but we found this does not benefit the streaming applications we are targeting. Data structures marked non-cacheable will not be cached and are accessed directly from memory. If the available size of shared memory per thread is less than *cacheLineSize* (i.e., too much shared memory has already been allocated by the application) then S-L1 is effectively disabled by assigning no cache lines to threads (i.e., *CLN* = 0).

To determine which data structures to cache, we evaluate the benefit of caching the data of each data structure using a short monitoring phase at runtime. In the monitoring phase, the core computation of the application is executed for a

<sup>5</sup>In this context, each argument to the GPU kernel that points to data is referred to as a data structure. For example, matrix multiply might have three arguments a, b and c referring to three matrices; each is considered a data structure.

short period of time, during which a software cache for each data structure and thread is simulated to count the number of cache hits. When the monitoring phase terminates, the *CLN* data structures with the highest cache hit counts will be marked so they are cached. The code required for the monitoring phase is injected into existing applications using straightforward compiler transformations.

## 3.2 Code Transformations

The compiler transforms the main loop(s) of the GPU kernel into two loop slices. The first loop slice is used for the monitoring phase, where the computation is executed for a short period of time using the cache simulator. After the first loop slice terminates, the data structures are ranked based on their corresponding cache hit counts, and the top *CLN* data structures are selected to be cached in S-L1. The second loop slice then executes the remainder of the computation using S-L1 for the top *CLN* data structures.

As an example, the following code:

```
//Some initialization
for(int i = start; i < end; i++) {
    char a = charInput[i];
    int b = intInput[i];

    int e = doComputation(a, b);
    intOutput[i] = e;
}
//Some final computation
```

is transformed into:

```
//Some initialization
cacheConfig_t cacheConfig;
int i = start;

//slice 1: monitoring phase
for(; (i < end) && (counter < THRESHOLD); i++, counter++) {
    char a = charInput[i];
    simulateCache(&charInput[i], 0, &cacheConfig);
    int b = intInput[i];
    simulateCache(&intInput[i], 1, &cacheConfig);

    int e = doComputation(a, b);
    intOutput[i] = e;
    simulateCache(&intOutput[i], 2, &cacheConfig);
}
calculateWhatToCache(&cacheConfig, availNumCacheLines);
//slice 2: rest of the computation
for(; i < end; i++)
{
    char a = *((char*) accessThroughCache(&charInput[i], 0,
                                         &cacheConfig));
    int b = *((int*) accessThroughCache(&intInput[i], 1,
                                       &cacheConfig));

    int e = doComputation(a, b);

    *((int*) accessThroughCache(&intOutput[i], 2,
                               &cacheConfig)) = e;
}
flush(&cacheConfig);
//Some final computation
```

### 3.2.1 Monitoring phase

In the monitoring loop, a call to `simulateCache()` is inserted after each memory access. This function takes as argument the address of the memory being accessed, a *data structure identifier*, and a reference to the *cacheConfig* object,

which stores all information collected during the monitoring phase. The *data structure identifier* is the identifier of the data structure accessed in the corresponding memory access, and is assigned to each data structure statically at compile time.

The pseudo code of `simulateCache()` is listed below. This function keeps track of which data is currently being cached in the cache line, assuming a single cache line is allocated for each thread and data structure, and it counts the number of cache hits and misses that occurred. To do this, `cacheConfig` contains, for each data structure and thread, an address variable identifying the memory address of the data that would currently be in the cache, and two counters that are incremented whenever a cache hit or miss occurs, respectively. On a cache miss, the address variable is updated with the memory address of the data that would be loaded into the cache line.

```
simulateCache(addr, accessId, cacheConfig) {
    addr /= CACHELINESIZE;

    if(addr == cacheConfig.cacheLine[accessId].addr)
        cacheConfig.cacheLine[accessId].hit++;
    else {
        cacheConfig.cacheLine[accessId].miss++;
        cacheConfig.cacheLine[accessId].addr = addr;
    }
}
```

The monitoring phase is run until sufficiently many memory accesses have been simulated so that the behavior of the cache can be reliably inferred. To do this, we simply count the number of times `simulateCache()` is called by each thread; once it reaches a predefined threshold for each thread, the monitoring phase is exited. This pre-defined threshold is set to 300 in our current implementation.<sup>6</sup>

### 3.2.2 Determining what to cache

In the general case, we mark the *CLN* data structures with the highest cache hit counts to be cached in S-L1. However, there are two exceptions. First, we distinguish between read-only and read-write data structures. Read-write data structures incur more overhead, since dirty bits need to be maintained and dirty lines need to be written back to memory. Hence, we give higher priority to read-only data structures when selecting which structures to cache. Currently, we select a read-write data structure over a read-only data structure only if its cache count rate is twice that of the read-only data structure, because accesses to read-write cache lines involve the execution of twice as many instructions on average.

Secondly, in our current implementation, we only cache data structures if it has a cache hit rate above 50%. A hit rate of more than 50% means that, on average, the cache lines are reused at least once after loading the data due to a miss.

<sup>6</sup>This method of statically setting the duration of monitoring phase works well for regular GPU applications such as the ones we are targeting, but more sophisticated methods may be required for more complex, irregular GPU applications. Moreover, while we only run the monitoring phase once, it may be beneficial to enter into a monitoring phase multiple times during a long running kernel to adapt to potential changes in the caching behavior.

We do this because otherwise the overhead of the software implementation will not be amortized by faster memory accesses.

### 3.2.3 Computation phase

In the second loop slice, the compiler replaces all memory accesses with calls to `accessThroughCache()`. This function returns an address, which will either be the address of the data in the cache, or the address of the data in memory, depending on whether the accessed data structure is cached or not. A simplified version of the function is as follows:

```
void* accessThroughCache(void* addr, int accessId,
                        cacheConfig_t* cacheConfig)
{
    if(cacheConfig.isCached[accessId] == NOT_CACHED) {
        return addr;
    }
    else {
        //If already cached, then simply return the
        //address within the cache line
        if(alreadyCached(addr, cacheCon-
fig.cacheLine[accessId])) {
            return &(cacheConfig.cachelines[accessId].
                data[addr % 16]);
        }
        //requested data is not in the cache, so,
        //before caching it we need to evict current data.
        else {
            //If not dirty, simply overwrite. If dirty,
            //first dump the dirty data to memory

            if(cacheConfig.cachelines[accessId].dirty) {
                dumpToMemory(cacheConfig.cachelines[accessId]);
            }
            loadNewData(addr, cacheCon-
fig.cachelines[accessId]);
            return &(cacheConfig.cachelines[accessId].
                data[addr % 16]);
        }
    }
}
```

S-L1 cache misses on cacheable data cause the eviction of an existing cache line to make space for the new target cache line. Modified portions of the current cache line are first written back if necessary; a bitmap (kept in registers) is used to identify which portions of the cache line are modified. This approach also guarantees that two different threads will not overwrite each others data if they cache the same line (in different S-L1 lines) and modify different portions of it.

A call to `flush()` is inserted after the second loop slice to flush the modified cache lines to memory and invalidate all cache lines before the application terminates.

Extra overhead can be avoided if the pointers to the data structures provided as arguments to the GPU kernel are not aliased. Programmers can indicate this is the case by including the `restrict` keyword with each kernel argument. If this keyword is not included then the caching layer will still work properly, albeit with extra overhead because it has to assume the pointers may be aliased, in which case the caching layer will need to perform data lookups in all cache lines assigned to the same thread for each memory access — even for memory accesses to uncached data structures.

## 3.3 S-L1 overheads

Our implementation of S-L1 introduces overheads for the monitoring phase, when determining what data structures

to cache and for each memory access, and when executing `accessThroughCache()` for each memory access.

Our experiments show that the performance overhead of the monitoring phase is relatively low — an average of less than 1% was observed in the 10 applications we experimented with (see Section 4.4). The overhead is low because the monitoring phase only runs for a short period of time and because the code of `simulateCache()` is straightforward and typically does not incur additional memory accesses since all variables used in `simulateCache()` are located in statically allocated registers. In terms of register usage, the monitoring phase requires three registers per data structure/simulated cache line: one for the mapped address of the cache line in memory and two to keep the cache hit and miss counters. These registers are only required during the monitoring phase and will be reused after the phase terminates.

The performance overhead of `calculateWhatToCache()` is negligible since it only needs to identify which *CLN* data structures have the highest hit counts, and typically, applications only access a few data structures.

Most of the overhead of the caching layer occurs in the function `accessThroughCache()`. For accesses to non-cached data structures, the performance overhead entails the execution of four extra machine instructions. However, accesses to cached data structures incur significantly more overhead in some cases; e.g., when evicting a cache line. Our experiments indicate that the caching layer increases the number of instructions issued by 25% on average over the course of the entire application (see Section 4.4). This overhead can indeed negatively impact the overall performance of an application if it is not amortized by the lower access times offered by S-L1, and the overhead is exacerbated if the application’s throughput is already limited by instruction-issue bandwidth.

In terms of register usage, `accessThroughCache()` requires three additional registers per data structure and thread: one for the memory address of the data currently being cached, one for the write bitmap (which also serves as the dirty bit), and one for the data structure identifier. (If the data structure is not cached, the value of the last register will be -1). As an optimization, we do not allocate bitmap registers for read-only data structures. Additionally, since data structures that are not cached do not access the bitmap and address registers, the compiler might spill them to memory, without accessing them later, thus reducing the register usage of uncached data structures to 1. The recent GPU architectures (e.g. *Kepler*) have 65,535 registers per SMX and can support at most 2,048 threads, in which case the S-L1 caching layer would, in the worst case, use up to 6% and 9% of the total number of available registers for cached read-only and read-write data structures, respectively.

## 3.4 Coherence considerations

Since each thread has its own private cache lines, cached data will not be coherent across cache lines of different threads. Thus, if two threads write to the same data item cached separately, the correctness of the program might be compromised. Fortunately, the loose memory consistency model

offered by GPUs makes it easy to maintain the same level of consistency for S-L1 accesses. We follow two simple rules to maintain the correctness of the program: (a) we flush the threads’ cache lines on *memory fence instructions* and (b) we do not cache the data of data structures that are accessed through atomic instructions.

Executing a *memory fence instruction* enforces all memory writes that were performed before the instruction to be visible to all other GPU threads before the execution of the next instruction. GPGPU programmers are required to explicitly use these instructions if the application logic relies on a specific ordering of memory reads/writes. We implement this by inserting a call to `flush()` immediately before each memory fence instruction, which flushes the contents of the modified cache lines to memory and invalidates the cache lines.

By executing an *atomic instruction*, a thread can read, modify, and write back a data in GPU memory atomically. We extract the data structures that might be accessed by atomic instructions at compile time and mark them as not cacheable.

## 4. EXPERIMENTAL EVALUATION

### 4.1 Experimental Setup

All GPU kernels used to evaluate S-L1 were executed on an Nvidia GeForce GTX Titan Black GPU connected to 6GB of GPU memory with a total of 2,880 computing cores running at 980MHz. As described in Section 2.1, the GTX Titan Black is from the Kepler family and has 15 streaming multiprocessors (SMXs), each with 192 computing cores, and 64KB of on-chip memory (of which 48KB is assigned to shared memory).

All GPU-based applications were implemented in CUDA, using CUDA toolkit and GPU driver release 7.0.28 installed on a 64-bit Ubuntu 14.04 Linux with kernel 3.16.0-33. All applications are compiled with the corresponding version of the *nvcc* compiler using optimization level three.

For each experiment, we ran the target application using different thread configurations, and only considered the configuration with the best execution time for reporting and comparison purposes.<sup>7</sup> Specifically, we tested each application using 512 different thread configurations, starting with 15 blocks of 128 threads (for a total of 1,920 threads) and increased the number of threads in 128 increments, up to 480 blocks of 1,024 threads (for a total of 480K threads).

### 4.2 S-L1 performance evaluation for GPU-local applications

We applied S-L1 to the ten streaming applications listed in Table 1. There is no standard benchmark suite for GPU streaming applications, so we selected 6 representative applications, 2 simple scientific applications (`MatrixMultiply` and `Kmeans`), and 2 extreme applications to stress test S-L1: `wc`, which has minimal computation (only counter increments) for each character access, and `upper`, which is similar

<sup>7</sup>GPGPU programmers typically experimentally run their applications with different thread configurations to determine the optimal number of threads and from then on run that configuration.

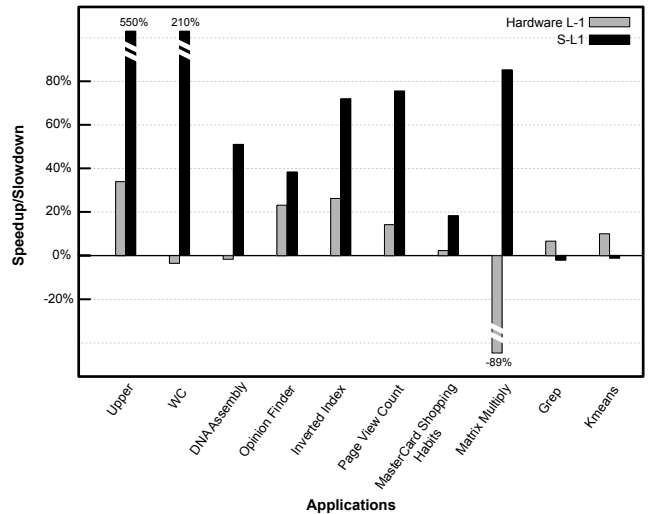


Figure 7: Speedup when using S-L1 relative to no L1 caching.

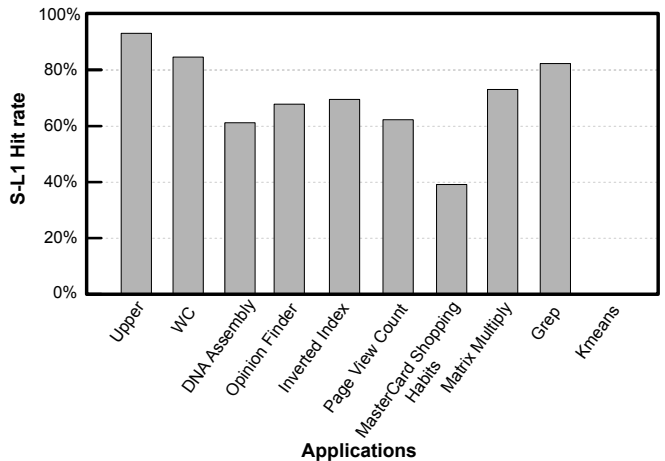


Figure 8: S-L1 hit rate.

to `wc` but may modify the characters. For each experiment, the data accessed by the applications is already located in GPU memory.

Figure 7 shows the performance of our 10 benchmark streaming applications when run with S-L1 and hardware L1 relative to the performance of the same applications run with no L1 caching (L2 cache is enabled in all cases). On average, the applications using S-L1 run 1.9 times faster than when they use the hardware L1 and 2.1 times faster than when run with no L1 caching.

With hardware L1, performance improves to at most 35% and in some cases degrades significantly. In particular, `wc`, `PageViewCount`, and `Matrix Multiply` exhibit slowdown. We attribute the poor performance to the extra DRAM transactions due to the constant thrashing of L1 cache lines: each cache miss results in four DRAM transactions (four 32-byte transactions to fill the 128-byte cache line), three transactions more than what is actually required to fulfill the requesting memory access instruction, a phenomenon originally observed by Jia et al. [8].



Application	Description	Used number of data structures
Upper	Converts all text in an input document from lowercase to uppercase.	2
WC	Counts the number of words and lines in an input document.	1
DNA Assembly	merges fragments of a DNA sequence to reconstruct a larger sequence [3].	3
Opinion Finder	analyzes the sentiments of tweets associated with a given subject (i.e. a set of given keywords) [24]	4
Inverted Index	Builds reverse index from a series of HTML files.	3
Page View Count	Counts the number of hits of each URL in a web log.	3
MasterCard Affinity	finds all merchants that are frequently visited by customers of a target merchant X [14]	3
Matrix Multiply	Calculates the multiplication of two input matrices. This is a naive version and does not use shared memory.	3
Grep	Finds the string matching a given pattern and outputs the line containing that string.	2 (1 in shared memory)
Kmeans	Partitions $n$ particles into $k$ clusters so that particles are assigned to the cluster with the nearest mean.	2 (1 in shared memory)

**Table 1:** Ten streaming applications used in our experimental performance evaluation and the number of data structures they use in their main loop. S-L1 determines the number of data structures to cache at runtime, which could vary from run to run depending on the available size of shared memory per thread (see Section 3.1).

With S-L1, some applications (e.g., `upper` and `wc`) run multiple times faster than with hardware L1, while other applications (e.g., `grep` and `kmeans`) experience slight slowdowns. The benefits obtained from S-L1 depends on a number of factors. First, the attained cache hit rate obviously has a large effect. Figure 8 depicts the S-L1 hit rate for all benchmarks. Overall, the hit rate is quite high, in part because most of the applications have high spatial locality (which is to be expected for streaming applications). As an extreme example, consider `wc`, where each thread accesses a sequence of adjacent characters, so each S-L1 miss is typically followed by 15 hits, given a 16 byte cache line. Kmeans is an exception: because the application allocates much of the shared memory for its own purposes, there is insufficient space for S-L1 cache lines, and hence the effective S-L1 hit rate is zero for this application.<sup>8</sup>

A second factor is the memory intensity of the applications; i.e., the ratio of memory access instructions to the total number of instructions executed. Some applications (e.g., `upper` and `wc`) are memory bound and hence benefit from S-L1. At the other extreme, `grep` doesn’t perform as well despite having a high cache hit rate, mainly because it becomes instruction throughput bound after applying S-L1 due to the application’s recursive algorithm. The benefits of the caching layer is negated by the extra instructions that need to be executed because of the software implementation of S-L1.

A third factor is the degree to which S-L1 enables extra productive thread parallelism, thus improving GPU core utilization. Figure 9 shows the number of *online* threads<sup>9</sup> that result in the best performance for each application with S-L1 and with hardware L1. Overall, applications perform best with a larger number of threads when using S-L1 compared to hardware L1, because hardware L1 leads to increased L1 and L2 cache thrashing.

<sup>8</sup>Because Kmeans allocates space in shared memory dynamically at run time, the compiler cannot know that there is not enough space for S-L1 cache lines — otherwise it potentially could have avoided adding the code required for S-L1. In practice, Kmeans would be run without S-L1, so it would not have to incur the S-L1 overheads.

<sup>9</sup>I.e., threads that run at the same time on all multiprocessors, the maximum of which can be 30K threads on our GPU.

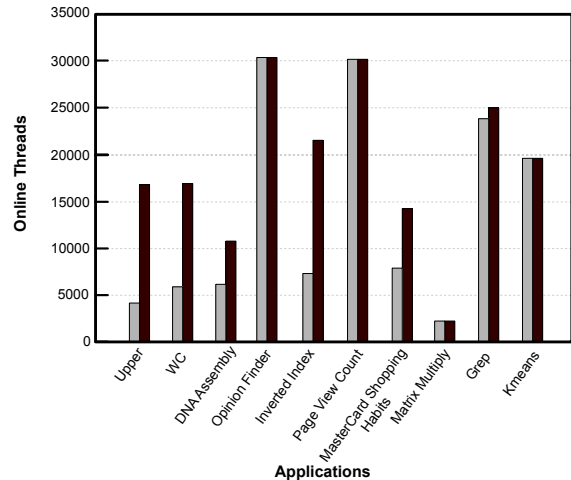


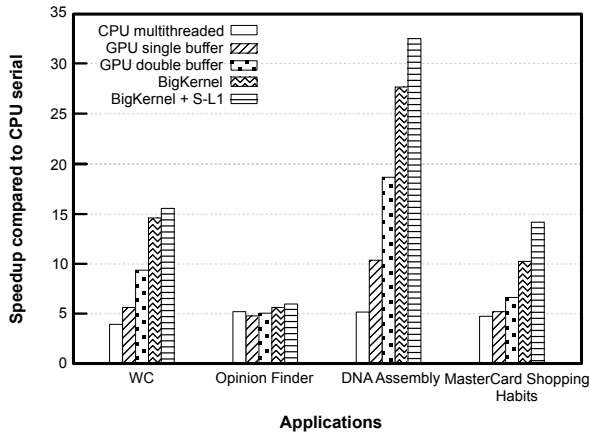
**Figure 9:** The optimal number of online threads (that leads to the best execution times) with and without S-L1.

### 4.3 Evaluation of S-L1 for data residing in CPU memory

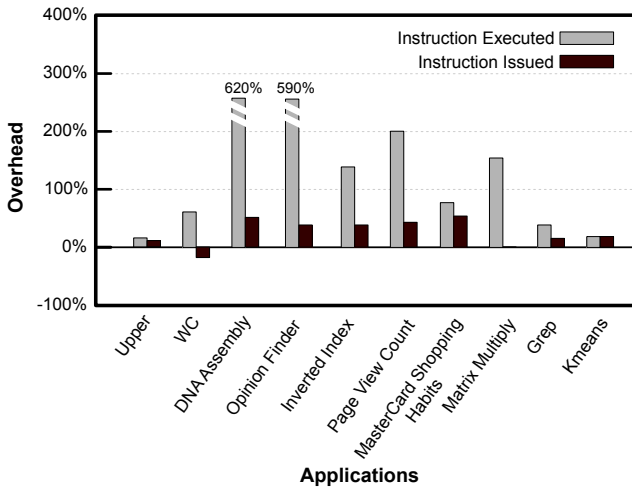
For big data-style applications, the data will not fit in GPU memory because of the limited memory size. Hence, in this subsection, we consider the performance of four applications with data sets large enough to not fit in GPU memory. We ran these applications under five different scenarios:

1. CPU multithreaded when run on a 3.7GHz Intel Core i7-4820K with 24GB of dual-channel memory clocked at 1.8 GHz;
2. GPU using a single buffer to transfer data between CPU and GPU;
3. GPU using state-of-the-art double buffering to transfer data between CPU and GPU;
4. GPU using BigKernel [14]; and
5. GPU using BigKernel combined with S-L1.

We selected to combine S-L1 with BigKernel in particular, because BigKernel is, to the best of our knowledge, the currently best performing system for data intensive GPU streaming applications [14].



**Figure 10:** Speedup of four GPU applications processing large data sets located in CPU memory relative to the CPU serial versions.



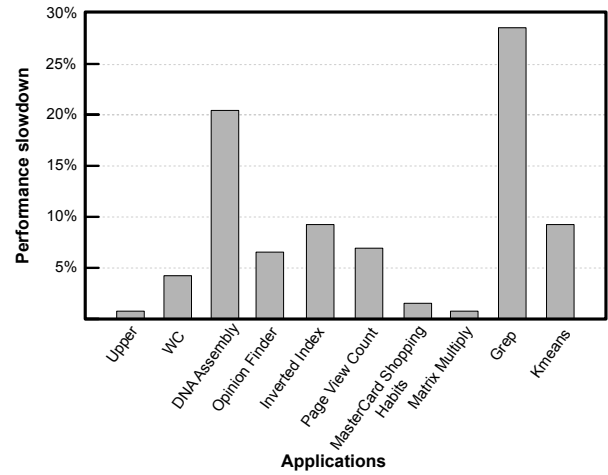
**Figure 11:** Extra instructions executed and issued (in %) due to S-L1.

Figure 10 shows the results. For all four applications, using BigKernel with S-L1 performs the best, and for all but one application the performance is an order of magnitude better than the multithreaded CPU version. Compared to BigKernel alone, BigKernel with S-L1 is 1.19X faster. Limits in thread parallelism is the primary reason BigKernel is prevented from performing better when combined with S-L1, because BigKernel requires the use of many registers.<sup>10</sup> As shown in Figure 9, one of the ways S-L1 improves performance is by allowing applications to efficiently exploit higher degrees of parallelism.

#### 4.4 S-L1 overheads

S-L1 has significant overhead because it is implemented in software. However, based on our experiments, the monitoring phase accounts for less than 1% of this overhead. After the monitoring phase, a minimum of 4 and potentially well over 100 extra instructions are executed for each memory access. Figure 11 depicts the increase in the number

<sup>10</sup>When a kernel uses high number of registers, an SMX will schedule fewer *online threads* to be able to provide them with the required number of registers.



**Figure 12:** Overhead of S-L1 when it is enabled but not used to cache data.

of instructions, both executed and issued, when using S-L1 compared to when using hardware L1. Executed instructions are the total number of instructions completed, while issued instructions also count the times an instruction is “replayed” because it encountered a long latency event such as a memory load.

The increase in the number of executed instructions is significant: 220% on average. The reason is obvious: each memory access instruction is transformed to additionally call a function that needs to be executed. On the other hand, the increase in the number of issued instructions is more reasonable: 25% on average. (For `wc` and `MatrixMultiply` the number of issued instructions actually decreases.) The reason issued instructions increase less than executed instructions is that S-L1 provides for improved memory performance, which reduces the number of required instruction replays.

To evaluate S-L1 overheads when accessing non-cached data structures, we ran our benchmarks with S-L1 enabled but all data structures marked as non-cacheable. Figure 12 shows that the overhead is 8% on average. The primary source of the overhead is attributed to executing the memory access function that is called for each memory access. As suggested in Section 4.2, one potential way to avoid this overhead is have the compiler not transform memory accesses to data structures that are found not worthy of caching – e.g. a data structure that is statically known to not exhibit any caching benefit.

#### 4.5 Effect of S-L1 cache line size

Figure 13 compares the overall performance of applications when using different variations of S-L1 using different cache line sizes. Specifically, we show the performance improvement/loss for 8-byte and 24-byte cache lines over 16-byte cache lines.<sup>11</sup>

In most cases, 16-byte cache lines seems to be best choice. As we described in Section 3.1, we believe this is mainly because

<sup>11</sup>We did not consider 32 as a potential cache line size since this size would not be able to support 2,048 threads given the maximum size of shared memory (i.e. 48KB).

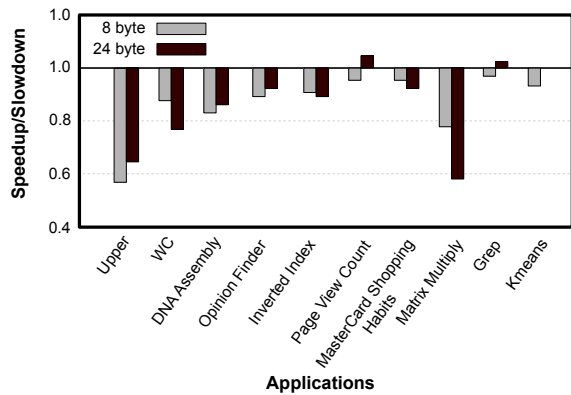


**Figure 13:** Slowdown/speedup when using 8B and 24B cache lines over using 16B cache lines.

16-bytes is the widest available load/store size on GPU ISA and hence, the entire cache line can be read/written with one memory access.

Decreasing the cache line size to 8-bytes impacts performance negatively in every case, since the cache then typically needs to execute the inserted memory access function twice as often for a fixed amount of streaming data to be processed by the application. Note that our benchmarks primarily consist of streaming applications that have high spatial locality and that consume most of the data in a cache lines.

Increasing the cache line size to 24-bytes also reduces performance in all but two cases, mainly because 24 bytes do not provide much additional benefit over 16 bytes, yet require two memory accesses to fill a cache line instead of one. For example to process 48 characters accessed sequentially, a 16B cache line results in 3 misses and thus 3 L2/DRAM accesses, whereas a 24B cache line results in 2 misses and thus 4 L2/DRAM accesses.

## 5. RELATED WORK

A large body of work focuses on using shared memory to increase the performance of applications in an application centric way [4, 10, 12, 17, 18, 22]. For instance, Nukada et al. propose an efficient 3D FFT that uses shared memory to exchange data efficiently between threads [15].

Other work studies more general approaches to harness the benefits of shared memory, typically by providing libraries or compile time systems that use shared memory as a scratch-pad to optimize the memory performance of applications [1, 7, 9, 13, 20, 26]. For instance CudaDMA provides a library targeting scientific applications that allows the programmer to stage data in shared memory and use the data from there [2]. A producer consumer approach is proposed where some warps only load the data in shared memory (producer) and others only compute (consumer). What we achieve with S-L1 can also be achieved with CudaDMA; however with CudaDMA the programmer must use the API manually, set the number of producer and consumer threads, and assign the proper size of shared memory to different threads.

Yang et al. propose a series of compiler optimizations, including vectorization and data prefetching, to improve the

bandwidth of GPU memory [26]. In particular, they provide a technique in which uncoalesced memory accesses are transformed to coalesced ones using shared memory for staging.

Other researchers have also studied the characteristics of GPU memory and GPU caches [5, 25]. Jia et al. characterize L1 cache locality in Nvidia GPUs and provide a taxonomy for reasoning about different types of access patterns and how they might benefit from L1 caches [8]. Tore et al. provide insights into how to tune the configuration of GPU threads to achieve higher cache hit rates and also offers an observation on how the L1 impacts a handful of simple kernels [19].

Li et al. suggested that register files are a better storage for thread-private data than shared memory [11]. As an experiment, we modified S-L1 to use register files for data storage instead of shared memory, but this led to poorer performance. The reason, we found, is that GPU registers are small (e.g. 4-bytes) and therefore, a cache-line spans multiple registers, which will cause the entire cache line (e.g. four registers) to be copied to local memory before a location of it is accessed, if the accesses are dynamic (i.e. not known at compile time) – which is the case in S-L1.

Finally, a number of potential architectural changes that could improve the GPU caching behavior have been proposed, including a recent study that analyzes potential coherent models for GPU L1 caches [16].

## 6. CONCLUDING REMARKS

By reverse-engineering the Nvidia GTX Titan Black through a series of experiments, we characterized the behavior of the memory hierarchy of modern GPUs. We showed that the bandwidth between off-chip memory and GPU SMXs is limited so that the latency of L2/DRAM accesses increases substantially the more memory intensive the application. We also showed that raw GPU compute power has been growing faster than the size of on-chip L1 caches, resulting in substantially increased L2/DRAM access latencies once the memory intensity of the application reached a threshold.

To address these issues, we proposed S-L1, a GPU level 1 cache which is implemented entirely in software using SMX shared memory. S-L1 determines, at run time, the proper size of cache, samples the effectiveness of caching the data of different data structures, and based on that information, decides what data to cache. Although the software implementation adds 8% overhead to the applications we tested on average, our experimental results show that this overhead is amortized by faster average memory access latencies for most of these applications. Specifically, S-L1 achieves speedups of between 0.86 and 4.30 (1.90 avg) over hardware L1 and between 0.95 and 6.50 (2.10 avg) over no L1 caching on ten GPU-local streaming applications. Combining S-L1 with BigKernel, the fastest known technique accelerating GPU applications processing large data sets located in CPU memory, we achieved speedups of between 1.07 and 1.45 (1.19 avg.) over BigKernel alone, and speedups of between 1.07 and 6.37 (3.7 avg.) over the fastest CPU multicore implementations.

While it is understandable that GPU designers need to pri-

oritize optimizations for graphical processing and maintain commodity pricing, we believe that our work provides some indications of how GPU designers could enhance current designs to make GPU designs more effective for data intensive GPGPU applications. The most straightforward enhancement is to significantly increase the size of the L1 — its current size only supports 0.18 cache lines per thread when applications run with the maximum number of online threads allowed. Another enhancement would be to allow on-chip cache geometry to be more configurable, particularly allowing the cache lines to be smaller.

In future work, we intend to reduce the overhead of S-L1 by relying more on the compile-time technology. Using compiler technology, we can avoid transforming memory accesses to data structures that are statically known to exhibit poor caching behavior. Moreover, if accesses to all data structures can be statically analyzed, the monitoring phase might also become unnecessary.

## 7. REFERENCES

- [1] M. M. Baskaran, U. Bondhugula, S. Krishnamoorthy, J. Ramanujam, A. Rountev, and P. Sadayappan. A Compiler Framework for Optimization of Affine Loop Nests for GPGPUs. In *Proceedings of the 22nd Annual International Conference on Supercomputing (ICS '08)*, pages 225–234, 2008.
- [2] M. Bauer, H. Cook, and B. Khailany. CudaDMA: Optimizing GPU Memory Bandwidth Via Warp Specialization. In *Proceedings of 2011 international conference for high performance computing, networking, storage and analysis*, page 12, 2011.
- [3] J. Chapman, I. Ho, S. Sunkara, S. Luo, G. Schroth, and D. Rokhsar. Meraculous: De Novo Genome Assembly with Short Paired-End Reads. *PLoS ONE*, page e23501, 2011.
- [4] S. Che, M. Boyer, J. Meng, D. Tarjan, J. W. Sheaffer, S.-H. Lee, and K. Skadron. Rodinia: A Benchmark Suite for Heterogeneous Computing. In *IEEE International Symposium on Workload Characterization (IISWC 2009)*, pages 44–54, 2009.
- [5] J. Gaur, R. Srinivasan, S. Subramoney, and M. Chaudhuri. Efficient Management of Last-level Caches in Graphics Processors for 3D Scene Rendering Workloads. In *Proceedings of the 46th Annual IEEE/ACM International Symposium on Microarchitecture (MICRO 46)*, pages 395–407, 2013.
- [6] C. Gregg and K. Hazelwood. Where is the Data? Why You Cannot Debate CPU vs. GPU Performance Without the Answer. In *Proceedings of IEEE Intl. Symp. on Performance Analysis of Systems and Software (ISPASS)*, pages 134–144, 2011.
- [7] F. Ji and X. Ma. Using Shared Memory to Accelerate MapReduce on Graphics Processing Units. In *IEEE International Symposium on Parallel & Distributed Processing (IPDPS 2011)*, pages 805–816, 2011.
- [8] W. Jia, K. A. Shaw, and M. Martonosi. Characterizing and Improving the Use of Demand-fetched Caches in GPUs. In *Proceedings of the 26th ACM international conference on Supercomputing (ICS 26)*, pages 15–24, 2012.
- [9] M. Khan, P. Basu, G. Rudy, M. Hall, C. Chen, and J. Chame. A Script-based Autotuning Compiler System to Generate High-performance CUDA Code. *ACM Transactions on Architecture and Code Optimization (TACO)*, pages 31:1–31:25, 2013.
- [10] F. Khorasani, K. Vora, R. Gupta, and L. N. Bhuyan. CuSha: Vertex-centric Graph Processing on GPUs. In *Proceedings of the 23rd International Symposium on High-performance Parallel and Distributed Computing (HPDC '14)*, pages 239–252, 2014.
- [11] C. Li, Y. Yang, H. Dai, S. Yan, F. Mueller, and H. Zhou. Understanding the tradeoffs between software-managed vs. hardware-managed caches in GPUs. In *2014 IEEE International Symposium on Performance Analysis of Systems and Software (ISPASS)*, pages 231–242, 2014.
- [12] C.-H. Lin, S.-Y. Tsai, C.-H. Liu, S.-C. Chang, and J.-M. Shyu. Accelerating String Matching Using Multi-threaded Algorithm on GPU. In *Global Telecommunications Conference (GLOBECOM 2010)*, pages 1–5, 2010.
- [13] M. Moazeni, A. Bui, and M. Sarrafzadeh. A Memory Optimization Technique for Software-managed Scratchpad Memory in GPUs. In *IEEE 7th Symposium on Application Specific Processors (SASP'09)*, pages 43–49, 2009.
- [14] R. Mokhtari and M. Stumm. BigKernel – High Performance CPU-GPU Communication Pipelining for Big Data-Style Applications. In *Proceedings of the IEEE 28th International Parallel and Distributed Processing Symposium (IPDPS '14)*, pages 819–828, 2014.
- [15] A. Nukada, Y. Ogata, T. Endo, and S. Matsuoka. Bandwidth intensive 3-D FFT kernel for GPUs using CUDA. In *International Conference for High Performance Computing, Networking, Storage and Analysis (SC 2008)*, pages 1–11, 2008.
- [16] I. Singh, A. Shriraman, W. Fung, M. O'Connor, and T. Aamodt. Cache Coherence for GPU Architectures. 2013.
- [17] M. A. Suchard, Q. Wang, C. Chan, J. Frelinger, A. Cron, and M. West. Understanding GPU programming for statistical computation: Studies in massively parallel massive mixtures. *Journal of Computational and Graphical Statistics*, pages 419–438, 2010.
- [18] J. Tölke and M. Krafczyk. TeraFLOP computing on a desktop PC with GPUs for 3D CFD. *International Journal of Computational Fluid Dynamics*, pages 443–456, 2008.
- [19] Y. Torres, A. Gonzalez-Escribano, and D. R. Llanos. Understanding the Impact of CUDA Tuning Techniques for Fermi. In *2011 International Conference on High Performance Computing and Simulation (HPCS)*, pages 631–639, 2011.
- [20] S.-Z. Ueng, M. Lathara, S. S. Baghsorkhi, and W. H. Wen-mei. CUDA-lite: Reducing GPU Programming Complexity. In *Languages and Compilers for Parallel Computing*, pages 1–15. 2008.
- [21] M. Ujaldon. Inside kepler. <http://gpu.cs.uct.ac.za/Slides/Kepler.pdf>, 2013.
- [22] J. P. Walters, V. Balu, S. Kompalli, and V. Chaudhary. Evaluating the Use of GPUs in Liver Image Segmentation and HMMER Database Searches. In *IEEE International Symposium on Parallel & Distributed Processing (IPDPS 2009)*, pages 1–12, 2009.
- [23] Wikipedia. Geforce 700 series — Wikipedia, the free encyclopedia. [http://en.wikipedia.org/wiki/GeForce\\_700\\_series](http://en.wikipedia.org/wiki/GeForce_700_series), 2013.
- [24] T. Wilson, P. Hoffmann, S. Somasundaran, J. Kessler, J. Wiebe, Y. Choi, C. Cardie, E. Riloff, and S. Patwardhan. OpinionFinder: a System for Subjectivity Analysis. In *Proceedings of HLT/EMNLP on Interactive Demonstrations*, pages 34–35, 2005.
- [25] H. Wong, M.-M. Papadopoulou, M. Sadooghi-Alvandi, and A. Moshovos. Demystifying GPU Microarchitecture Through Microbenchmarking. In *2010 IEEE International Symposium on Performance Analysis of Systems Software (ISPASS)*, pages 235–246, 2010.
- [26] Y. Yang, P. Xiang, J. Kong, and H. Zhou. A GPGPU Compiler for Memory Optimization and Parallelism Management. In *Proceedings of the 2010 ACM SIGPLAN Conference on Programming Language Design and Implementation (PLDI '10)*, pages 86–97, 2010.